iScience

CellPress
OPEN ACCESS

Article

TRPV6 is a potential regulator of bone resorption in bone loss induced by estrogen deficiency

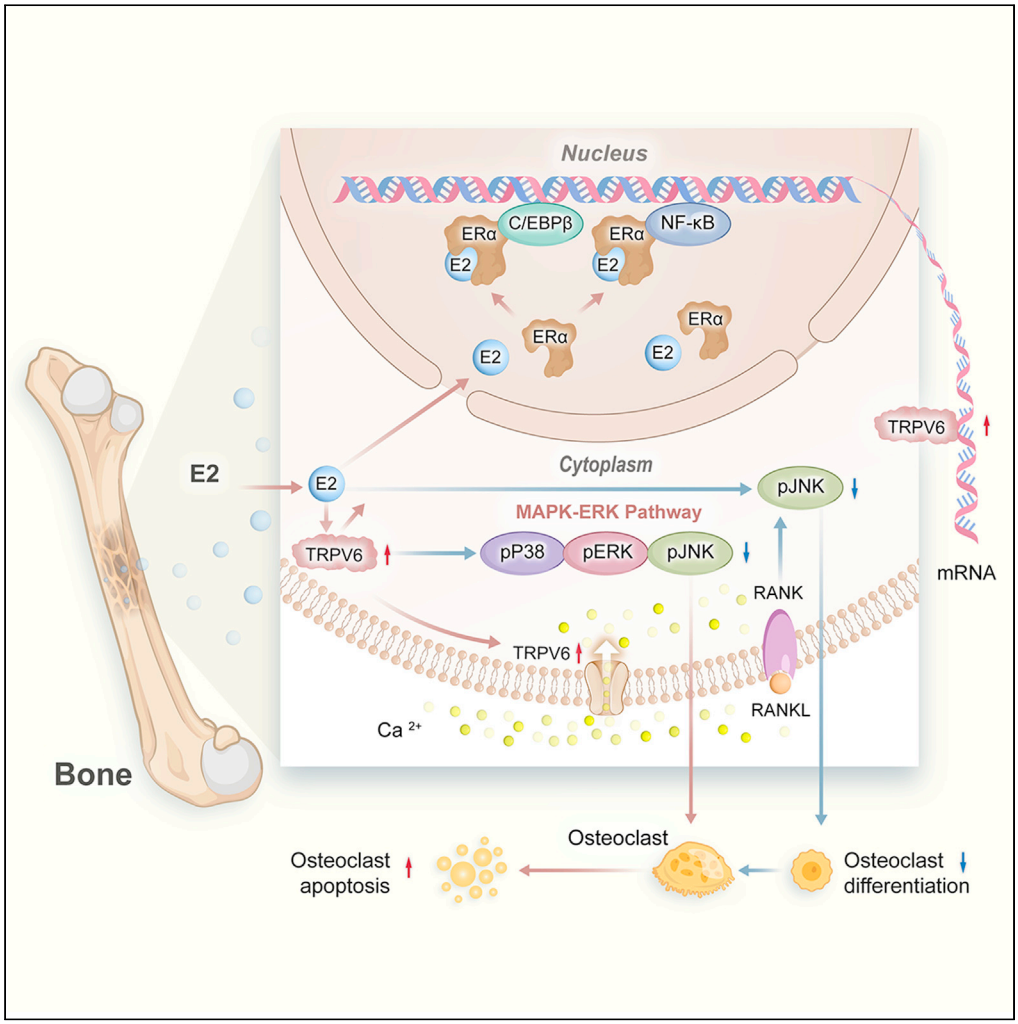

Jun Ma, Jiajia Lu, Zhibin Zhou, Nan Lu, Jia He, Lei Zhu, Tianwen Ye

yetianwenvip@126.com (T.Y.)
hejia64smmu@163.com (J.H.)
hailangzhulei@smmu.edu.cn (L.Z.)

Highlights

E2 induces Trpv6 expression in osteoclasts

TRPV6 was involved in the effect of E2-mediated osteoclast function

E2 regulates the transcription of Trpv6 through Erα in osteoclasts

Ma et al., iScience 24, 103261
November 19, 2021
https://doi.org/10.1016/j.isci.2021.103261

iScience

CellPress
OPEN ACCESS

Article

TRPV6 is a potential regulator of bone resorption in bone loss induced by estrogen deficiency

Jun Ma,[1,2,4] Jiajia Lu,[1,4] Zhibin Zhou,[3,4] Nan Lu,[1,4] Jia He,[2,*] Lei Zhu,[1,*] and Tianwen Ye[1,5,*]

SUMMARY

The precise effect of estrogen (E2) on osteoclast function is still poorly understood. The aim of this study was to investigate the potential role of transient receptor potential vanilloid 6 (TRPV6) in E2-mediated osteoclast function and to characterize the relevant underlying mechanisms. Here, we found that Trpv6 is drastically decreased in ovariectomy operation animals and the administration of E2 results in an increased expression of Trpv6 in osteoclasts. In contrast, Trpv6 depletion significantly blocked the inhibitory effects of E2 on bone resorption activity, and silencing Trpv6 alleviated E2-induced osteoclast apoptosis. In addition, we found that E2 regulates the transcription of Trpv6 through ERα, by interacting with C/EBPβ and NF-κB. Chip assay analysis indicated that C/EBPβ regulates Trpv6 transcription by binding to Trpv6 promoter fragments −1,866 nt to −1,761 nt and −2,685 nt to −2,580 nt, whereas NF-κB binds to the −953 nt to −851 nt region. We conclude that TRPV6 has a significant effect on E2-mediated osteoclast function.

INTRODUCTION

Osteoporosis is a common global metabolic bone disease characterized by decreased bone mineral density and bone mass (Klein-Nulend et al., 2015; Ma et al., 2019). Estrogen (E2) plays an important role in regulating bone metabolism and maintaining normal bone mass, and the lack of E2 leads to osteoporosis in most postmenopausal women (Hemmatian et al., 2017; Denger et al., 2008). Although it has been confirmed that osteoblasts, osteoclasts, and osteocytes all respond to E2, the increase of osteoclast formation and bone resorption activity caused by E2 deficiency is considered to have the central role in postmenopausal osteoporosis (Teitelbaum, 2000). As an important target of the effects of E2 in bone tissue cells, osteoclasts mainly originate from hematopoietic stem cells and monocytes, and their differentiation and activation are regulated by many factors (Ikebuchi et al., 2018; Kong et al., 1999). The macrophage colony-stimulating factor (M-CSF) and receptor activator of NF-κB ligand (RANKL) are the most critical molecules for osteoclastogenesis (Karsenty, 2006; Jeong et al., 2018). Numerous studies have indicated that E2 can act directly on osteoclast precursors to inhibit their differentiation (Mundy, 2007; Shevde et al., 2000). However, the precise molecular events underlying the effect of E2 on osteoclast differentiation need to be better understood.

Calcium ion (Ca^{2+}) channels are also essential for osteoclast differentiation and bone resorption (Masuyama et al., 2008). Previous findings indicate that RANKL induces oscillatory changes in intracellular Ca^{2+} concentrations and activates nuclear factor of activated T cells c1 (NFATc1), resulting in osteoclast-specific gene transcription to induce osteoclast differentiation (Hasegawa et al., 2010; Kim et al., 2010). Transient receptor potential vanilloid 6 (TRPV6) is a family of calcium transport proteins (Schoeber et al., 2007), which recent studies have found is involved in the regulation of bone metabolism (Chen et al., 2014a, 2014b; Bary, 2000; Beggs et al., 2019; Barthel et al., 2007). Our previous research indicates that TRPV5, which has homology as high as 66% with TPRV6, contributes to the process of E2-inhibited osteoclast differentiation and bone resorption activity (Chen et al., 2014a, 2014b). Because TRPV6-mediated Ca^{2+} influx is the key pathway for osteoclast differentiation induced by RANKL, and because Ca^{2+} channels are important targets for E2 to exert biological effects, we speculate that the regulatory effect of E2 on osteoclast formation and bone resorption may be related to calcium channel TRPV6 and TRPV6 may be the target gene that E2 affects during osteoclast function regulation.

[1]Department of Orthopedic, Changzheng Hospital, Naval Medical University, 415 Fengyang Road, Huangpu District, Shanghai, China

[2]Department of Health Statistics, Naval Medical University, 800 Xiangyin Road, Shanghai, China

[3]Department of Orthopedic Surgery, General Hospital of Northern Theater Command, No.83, Wenhua Road, Shenyang 110016, China

[4]These authors contributed equally

[5]Lead contact

*Correspondence: yetianwenvip@126.com (T.Y.), hejia64smmu@163.com (J.H.), hailangzhulei@smmu.edu.cn (L.Z.)

https://doi.org/10.1016/j.isci.2021.103261

In the current study, we investigated the mechanisms by which TRPV6 affects E2-mediated osteoclast differentiation and activity. Our results indicate that TRPV6 plays an important role in E2-mediated osteoclast formation, bone resorption activity, and osteoclast apoptosis. Further studies found that C/EBPβ and NF-κB contribute to the transcriptional activation of E2-ERα-mediated TRPV6 expression.

RESULTS

Estrogen deficiency leads to osteoporosis and increased bone resorption *in vivo*

Ovariectomized mice were used in this study to observe the role of endogenous E2 deficiency in bone metabolism. To examine whether the ovariectomized (OVX) mouse model was successfully generated, we compared the levels of plasma E2 in SHAM mice and OVX mice. The results indicated that plasma E2 concentrations were significantly depleted in OVX mice (Figure 1A). E2 deficiency following ovariectomy resulted in lowered bone mineral density (BMD) (Figure 1B). Representative μCT images of trabecular bone are presented in Figure 1C. TRAP staining in the bone sections further revealed the effect of E2 depletion on presence of osteoclasts (Figure 1D). Quantification showed that the number and surface area of osteoclasts in OVX mice were significantly higher than in SHAM mice (Figure 1E). In addition, compared with SHAM mice, OVX mice had higher levels of CTX-I and TRAP5b in plasma (Figures 1F and 1G). To summarize, these results confirmed that E2 deficiency leads to osteoporosis and increased bone resorption *in vivo*.

The effect of estrogen on Trpv6 expression in osteoclasts

Our previous study has revealed that Trpv6, which was distributed on the cell membrane of osteoclasts, acted as a negative regulator for osteoclast differentiation and function (Ma et al., 2021). To test whether E2 levels affect Trpv6 expression in osteoclasts, *Trpv6* mRNA levels were measured in osteoclasts from OVX and SHAM mice. The levels of *Trpv6* mRNA were considerably downregulated in the osteoclasts from OVX mice compared with SHAM mice (Figure 2A). Next, osteoclast precursors from normal mice were incubated with 10^{-8}M E2 at different time points. We found that *Trpv6* mRNA showed time-dependent increases following 24 and 48 h exposure to E2 compared with the control group (Figure 2B). These results were further supported by western blot analyses, which indicated that Trpv6 expression was decreased in the osteoclasts of OVX mice compared with SHAM mice (Figure 2C). Additionally, the expression of Trpv6 in the osteoclasts incubated with E2 increased in a time-dependent manner compared with the control group (Figure 2D). Taken together, these results strongly suggest that E2 induces Trpv6 expression in osteoclasts.

Silencing Trpv6 alleviates the inhibiting effect of estrogen on osteoclast differentiation and fusion

To further verify the role of Trpv6 on E2's regulation of osteoclasts, we silenced the *Trpv6* gene in osteoclasts using lentivirus transfection. Almost all cells expressed GFP, indicating that the lentivirus transfection rate was more than 95% (Figure 3A). PCR and western blotting confirmed that Trpv6 was effectively silenced (Figures 3B and 3C). Next, F-actin ring staining was applied in osteoclasts infected with Lenti-siRNA-TRPV6 under 10^{-7} M E2 and 50 ng/mL RANKL for 7 days. The results showed that E2 significantly inhibited osteoclast formation, which was alleviated by silencing trpv6 (Figures 3D and 3E). In accordance with the results of F-actin ring staining, results of the TRAP staining assay revealed that the number of $TRAP^{+}$ multinucleated osteoclasts incubated with E2 was significantly decreased. However, the silencing of Trpv6 significantly alleviated the inhibitory effect of E2 on osteoclast differentiation (Figures 3F and 3G). The mRNA levels of *cathepsin k, DC-STAMP, Atp6v0d2*, and *TRAP* were all decreased in osteoclasts incubated with E2, which was attenuated by silencing trpv6 (Figures 3H–3K). Mechanistically, E2 inhibits the RANKL-induced osteoclast differentiation through c-Jun N-terminal kinase. To further verify the role of TRPV6 on E2/RANKL/c-Jun, we silenced the *Trpv6* gene in osteoclasts incubated with E2. The levels of phosphorylation markers p-JNK/JNK were measured by western blotting. The results indicated that the ratios of p-JNK/JNK were decreased in osteoclasts treated with E2, which was attenuated by silencing Trpv6 (Figure 3L). The above results strongly suggest that silencing Trpv6 alleviates the inhibiting effect of E2 on osteoclast differentiation and fusion.

Trpv6-mediated Ca^{2+} influx is involved in the promotion effect of estrogen on osteoclast apoptosis

To investigate how Trpv6 mediates the effect of E2 on osteoclast apoptosis, we silenced Trpv6 expression in osteoclasts using Lenti-siRNA-TRPV6. AnnexinV-FITC/PI double staining was first used to examine cell apoptosis. The results indicated that E2 induced condensed and fragmented nuclei, which is characteristic

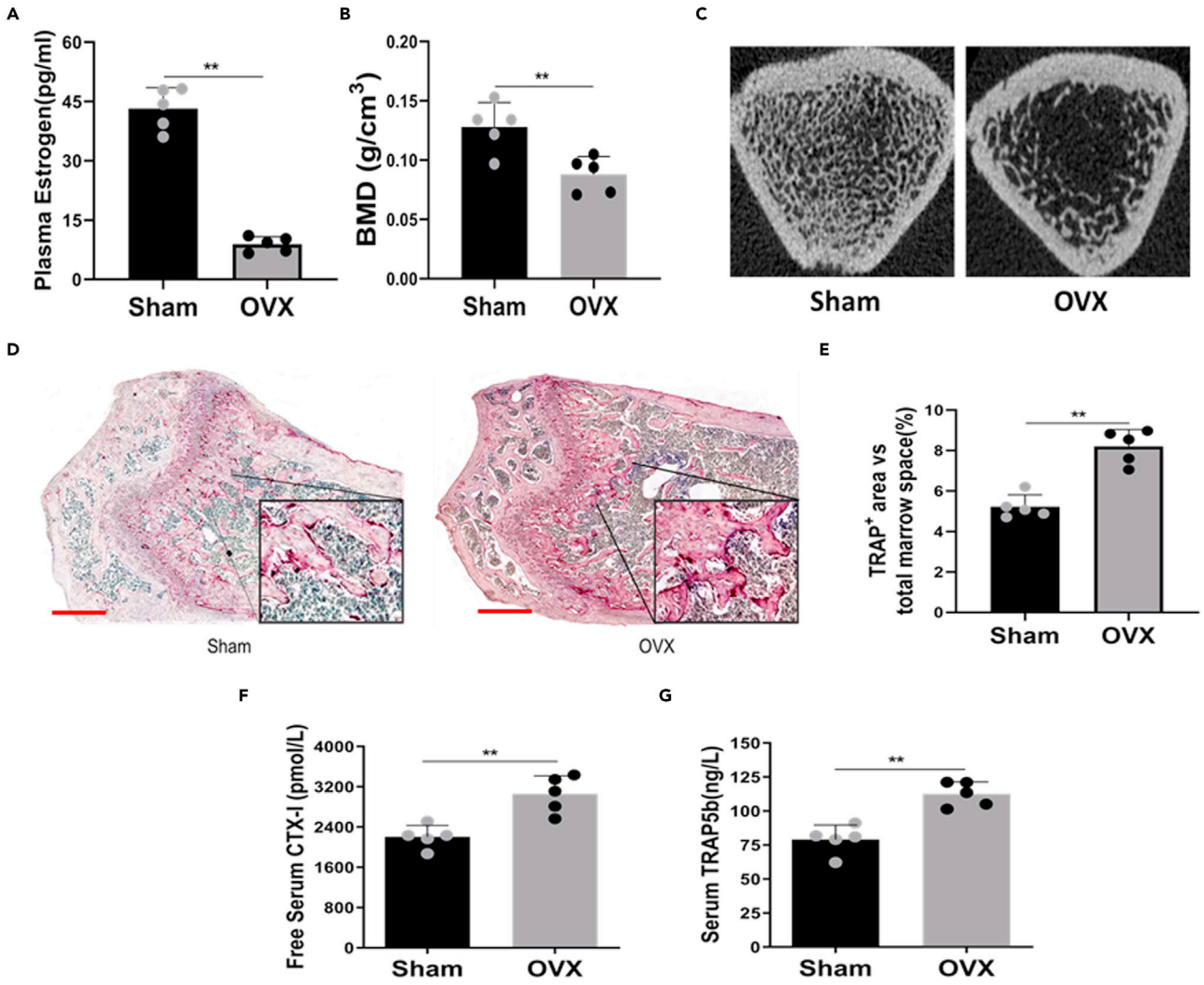

Figure1. Regulation of osteoclasts differentiation by estrogen *in vivo* and the effect of estrogen on TRPV6 expression in osteoclasts

(A) Plasma estrogen concentrations in SHAM mice and OVX mice were determined. n = 5, t = 13.56, **p<0.01.

(B) BMD in the distal end of the intact femurs of each experimental group. n = 5, t =3.449, **p<0.01.

(C) Representative figures of micro-CT analysis of the distal end of intact femurs from SHAM mice and OVX mice.

(D) Histologic sections of femurs stained for TRAP activity. Scale bars, 200 μm.

(E) Quantitative analysis of TRAP-stained area in femur sections of mice. n = 5, t = 4.89, **p<0.01.

(F) Serum levels of CTX-I of SHAM mice and OVX mice. n = 5, t = 4.42, **p<0.01.

(G) Serum levels of TRAP5b of SHAM mice and OVX mice. n = 5, t = 5.37, **p<0.01.

(A, B, E, F, and G) Results illustrate mean ± SD of n = 5, Statistical differences were determined by two-tailed non-paired Student's t test. Only statistically significant differences are illustrated. **p<0.01.

of apoptosis. However, these changes were significantly attenuated when Trpv6 was silenced (Figures 4A and 4B). In addition, total intracellular Ca^{2+} levels were measured in terms of relative fluorescence using Fluo-4AM 48 h after RANKL was added. Estrogen treatment significantly increased the levels of intracellular Ca^{2+}, but this increase was attenuated for cells where Trpv6 was silenced (Figures 4C and 4D). These results indicated that Trpv6 allows calcium influx, which leads to E2-induced apoptosis. Next, a Caspase-3 activity assay was applied because Caspase-3 plays an important role in the process of apoptosis. The results showed that a significant increase in Caspase-3 activity was observable in cells treated with E2, whereas it was reduced by the silencing of Trpv6 (Figure 4E). The BCL2/BAX ratio determines whether a cell will undergo apoptosis. Levels of BCL2 and BAX in osteoclasts were analyzed by western blot. The results showed that the Bcl-2/Bax ratio was decreased in osteoclasts treated with E2, but this decrease was attenuated for

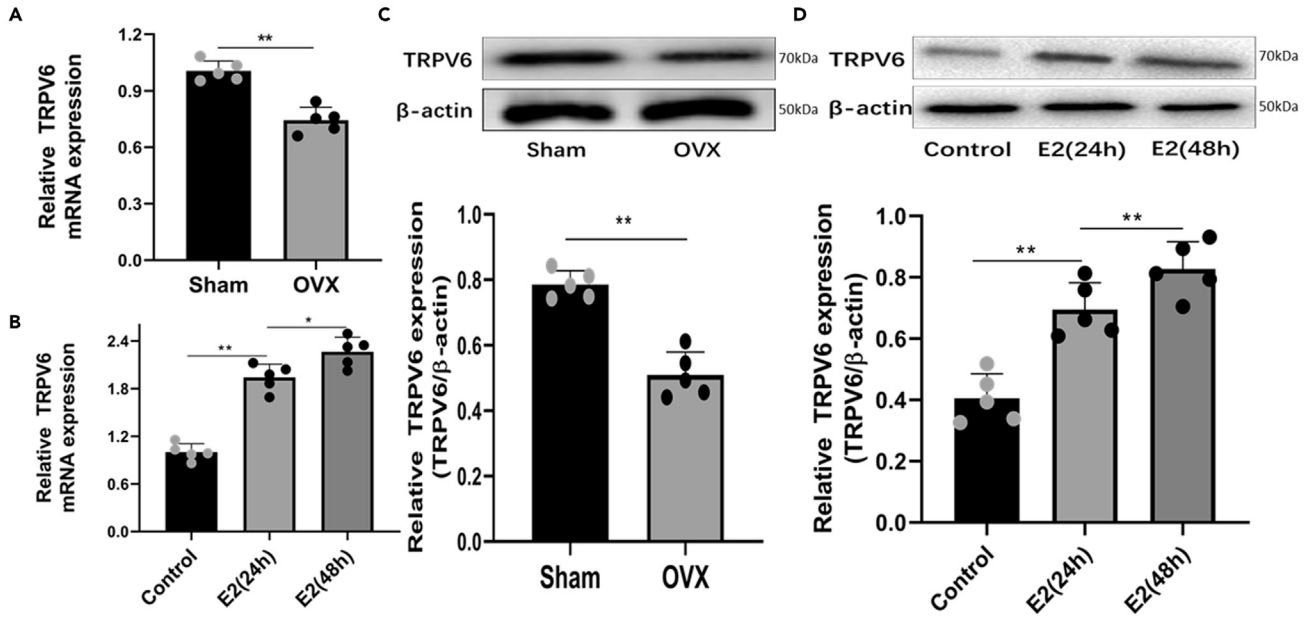

Figure2. The effect of estrogen on Trpv6 expression in osteoclasts

(A) Real-time RT-PCR analysis of TRPV6 mRNA expression in osteoclast from SHAM mice and OVX mice. n = 5, t = 6.71, **p<0.01.

(B) Real-time RT-PCR analysis of TRPV6 mRNA expression in osteoclasts precursors treatment with or without estrogen for 24 and 48 h. n = 5, F = 88.05, *p<0.05, **p<0.01.

(C) Western blot analysis of TRPV6 expression in osteoclasts from SHAM mice and OVX mice. n = 5, t = 7.55, **p<0.01.

(D) Western blot analysis of TRPV6 expression in osteoclasts precursors treatment with or without estrogen for 24 and 48 h. n = 5, F = 31.64, **p<0.01.

(A and C) Results illustrate mean ± SD of n = 5. Statistical differences were determined by two-tailed non-paired Student's t test. Only statistically significant differences are illustrated. **p<0.01. (B and D) Results illustrate mean ± SD of n = 5. Statistical differences were determined by one-way ANOVAs, and post hoc for multiple testing was corrected by Tukey method. Only statistically significant differences are illustrated. *p<0.05, **p<0.01.

cells where Trpv6 was silenced (Figure 4F). These results were further confirmed by TUNEL staining (Figure 4G). The above results strongly suggest that E2 stimulates osteoclast apoptosis by increasing Trpv6 expression.

Trpv6 induces osteoclast apoptosis by inhibiting the MAPK-ERK pathway

To further explore the role of Trpv6 and the mechanisms by which it affects osteoclast apoptosis, we silenced the *Trpv6* gene in osteoclasts using lentivirus transfection. AnnexinV-FITC/PI double staining results indicated that Trpv6 induced osteoclast apoptosis (Figures 5A and 5B). In addition, a significant decrease in Caspase-3 activity was observed following Trpv6 silencing in osteoclasts (Figure 5C). Furthermore, the levels of phosphorylated markers p-ERK/ERK, p-P38/P38, and p-JNK/JNK in the MAPK-ERK pathway were measured using western blotting. The results showed that the ratios of p-ERK/ERK, p-P38/P38, and p-JNK/JNK were increased following Trpv6 silencing in osteoclasts (Figures 5D–5G). Next, we used MEK inhibitor PD98059 to block the MAPK-ERK signaling pathway, and western blotting results revealed that there was no significant difference in the level of p-ERK/ERK when Trpv6 was silenced versus when it was not (Figures 5H–5I). The above results strongly suggest that Trpv6 promotes osteoclast apoptosis by inhibiting the MAPK-ERK pathway.

ERα is involved in the regulation of Trpv6 expression by E2

To examine the roles of two types of ER, ERα and ERβ, in E2-induced Trpv6 expression in osteoclasts, ERα and ERβ were separately silenced using Lenti-siRNA-ERα and Lenti-siRNA-ERβ. PCR and western blot analysis of ERα and ERβ expression confirmed that the deletions were effective (Figures 6A–6D). After being incubated with E2 under 50 ng/mL RANKL for 2 days, Trpv6 expression was measured in osteoclasts with depleted ERα or ERβ. The results of western blot and qRT-PCR showed that silencing ERα significantly reduced the stimulating effect of E2 on Trpv6 expression. However, silencing ERβ did not affect E2-induced Trpv6 expression (Figures 6E–6H). These results indicate that E2 regulates the expression of Trpv6 mainly through ERα. Subsequently, we assessed the expression of ERα and Trpv6 by immunofluorescence, and

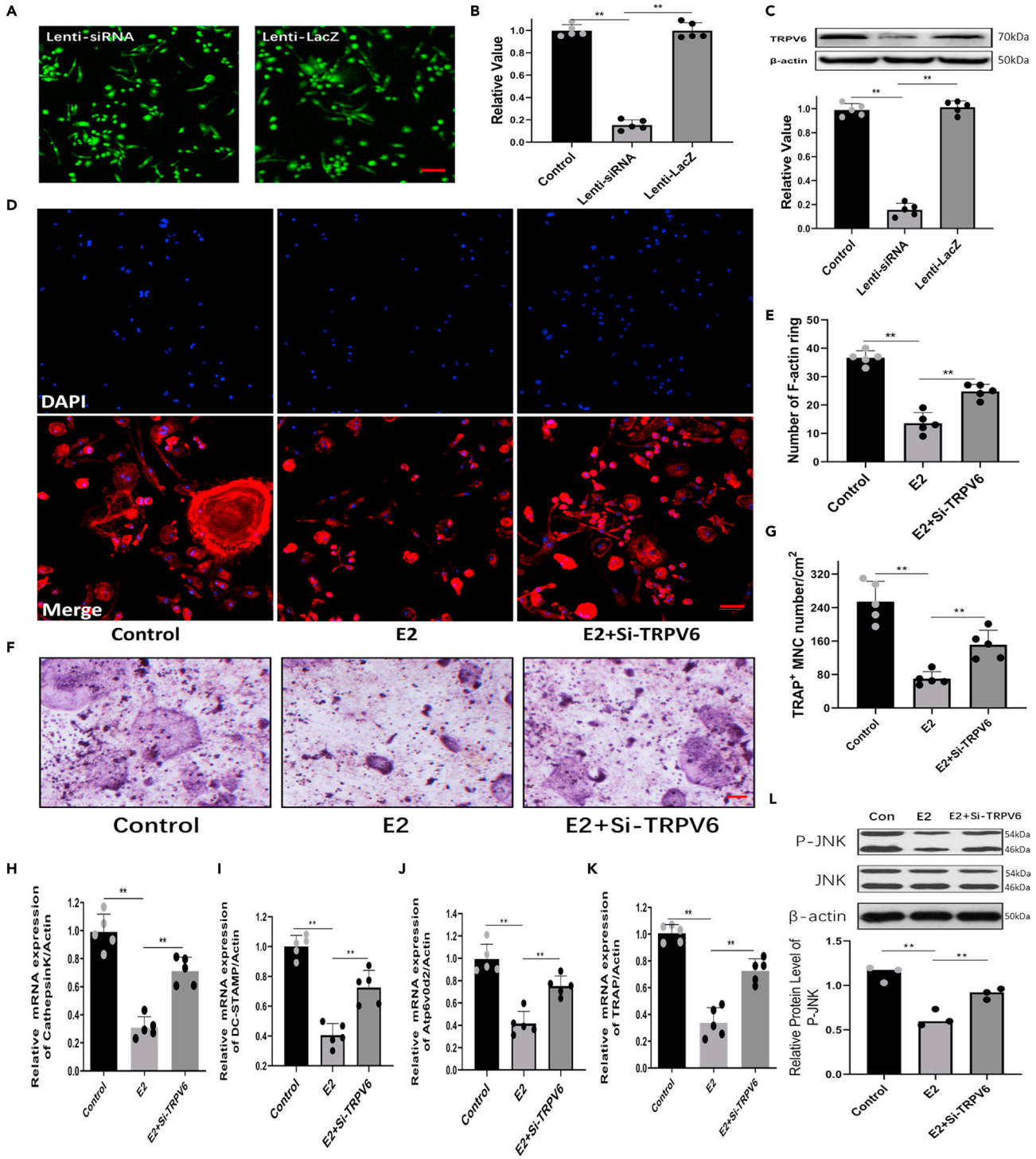

Figure3. Depletion of TRPV6 disturbs the inhibitory effect of estrogen on osteoclast differentiation and bone resorption activity

(A) All cells expressed GFP, showing that the cells were infected by lentivirus. Scale bars, 20 μm.

(B and C) Verified TRPV6 knockdown effect by lentivirus-mediated transduction of osteoclasts precursors. n = 5, **p<0.01.

(D) F-actin ring staining was performed to estimate the effect of TRPV6 on E2-inhibited osteoclastic bone resorption. Scale bars, 20 μm.

(E) Summarized data showed that depletion of TRPV6 significantly alleviated E2-decreased number of F-actin ring. n = 5, F = 75.44, **p<0.01.

(F) TRAP stain was performed to estimate the effect of TRPV6 on E2-inhibited osteoclastic bone resorption. Scale bars, 20 μm.

Figure3. *Continued*

(G) Summarized data showed that depletion of TRPV6 significantly alleviated E2-decreased resorption pit formation by osteoclasts. n = 5, F = 33.48, **p<0.01.

(H–K) QRT-PCR analysis of osteoclasts formation-specific genes, Cathepsin K, DC-STAMP, Atp6v0d2, and TRAP in cells treated with or without estrogen for 96 h and transfection with lentivirus-siRNA targeting TRPV6. n = 5, **p<0.01.

(L) The ratio of p-JNK/JNK was measured by western blot in osteoclast treated with E2 and infected with Lenti-siRNA-TRPV6 or not under RANKL for 30 min n = 3, **p<0.01.

(B, C, E, G, and H–K) Results illustrate mean ± SD of n = 5. Statistical differences were determined by one-way ANOVAs, and post hoc for multiple testing was corrected by Tukey method. Only statistically significant differences are illustrated. **p<0.01. (L) Results illustrate median of n = 3. Statistical differences were determined by Kruskal-Wallis test and corrected for multiple testing by Bonferroni. Only statistically significant differences are illustrated. **p<0.01.

results showed that osteoclasts expressed high levels of Trpv6 and ERα in the membrane and cytoplasm (Figure 6I).

Trpv6 is regulated by the transcription factor C/EBPβ and NF-κB

To further explore the mechanisms by which E2 promotes Trpv6 expression in osteoclasts, we used the online bioinformatical software program JASPAR (http://jaspar.genereg.net/cgi-bin/jaspar_db.pl) to analyze the promoter region of Trpv6; we identified the potential sites of C/EBPβ and NF-κB binding (Figure S1). Next, serial truncations of Trpv6 promoter were cloned into a pGL3-basic vector, and these constructs were transfected into osteoclasts. Cells were then treated with E2, and luciferase activity was measured, where higher activity measures indicate that the relevant regulatory element was important for the transcription of Trpv6 (Figure 7A). Then we overexpressed or silenced C/EBPβ and NF-κB in osteoclasts and verified the interference effect using PCR and western blot (Figures 7B–7F). Luciferase activity was measured after treatment with E2. Results showed that C/EBPβ and NF-κB knockdown significantly reduced luciferase activity (Figure 7G), whereas C/EBPβ and NF-κB overexpression significantly increased luciferase activity (Figure 7H). We next used a chromatin immunoprecipitation (ChIP) assay to examine whether the binding site was responsive to the C/EBPβ and NF-κB-mediated Trpv6 transcriptional activation that resulted from E2. Our results showed that C/EBPβ binds to the −1,866 nt to −1,761 nt and/or −2,685 nt to −2,580 nt fragments on the Trpv6 promoter in osteoclasts (Figures 7I and 7J), whereas the NF-κB-binding site is located at −953 nt to −851 nt on the trpv6 promoter in osteoclasts (Figures 7K and 7L). These findings indicate that the up-regulation of TRPV6 is mediated by C/EBPβ and NF-κB in E2-treated osteoclasts.

DISCUSSION

Bone is an important target tissue of E2. The inhibitor effects of E2 on osteoclast differentiation and bone resorption is a key mechanism underpinning postmenopausal osteoporosis (Klein-Nulend et al., 2015; Manolagas et al., 2013). However, the cellular and molecular mechanisms by which E2 deficiency increases osteoclastic bone resorption are not well specified. In the present study, we found that TRPV6 plays an important role in E2-inhibited osteoclast differentiation and activity. Our results provide key insights into the effect and mechanisms underlying TRPV6-dependent differentiation, bone resorption, and apoptosis in osteoclasts exposed to E2.

RANKL-evoked $[Ca^{2+}]i$ oscillations play a switch-on role in osteoclast differentiation through NFATc1, NFATc1 activation pathway that triggers osteoclast-specific gene expression (Kim et al., 2010). Both Ca^{2+} oscillation/calcineurin-dependent and -independent signaling pathways contributed to NFATc1 activation, resulting in efficient osteoclastogenesis (Kuroda et al., 2008). As an important member of the TRPV subfamily, the highly selective epithelial Ca^{2+} channel TRPV5 is essential for proper osteoclastic bone resorption (Eerden et al., 2005). TRPV5 deficiency leads to an increase in osteoclast size and number, in which Ca^{2+} resorption is nonfunctional (Chamoux et al., 2010). TRPV6, which shares 75% homology with TRPV5, participates in the regulation of intracellular Ca^{2+} concentration. Our previous research found that TRPV6 is highly expressed in human and mouse osteoclasts, and it is mainly distributed in the membrane pseudopodia, which is involved in the regulation of osteoclast differentiation and bone resorption (Chen et al., 2014a, 2014b). *Lieben et al* found that the bone mass of *trpv6* knockout mice decreased significantly and the bone resorption capacity of mice was significantly enhanced (Lieben et al., 2010). *Van der Eerden et al*. used knockin technology to breed $Trpv6^{D541A/D541A}$ mice with inactivated TRPV6 function. This study found that the bone mineralization ability of $Trpv6^{D541A/D541A}$ mice did not change (van der Eerden et al., 2012). However, no previous studies have reported whether TRPV6 is involved in the process of E2-regulated osteoclast differentiation and bone resorption. Our study is the first to report the effect of E2 on TRPV6 expression during osteoclastogenesis. We found that E2 induces TRPV6 expression in

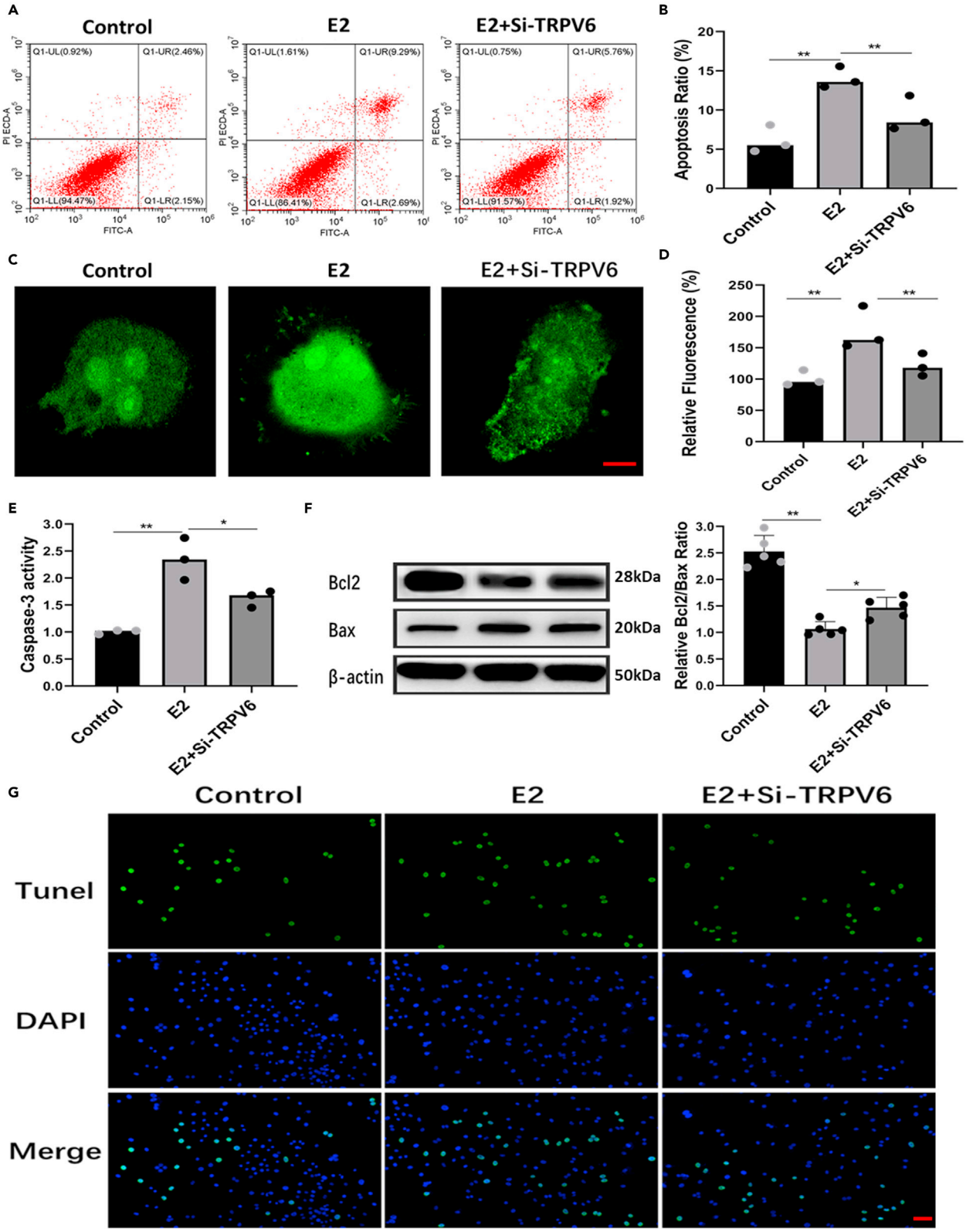
A
Control
E2
E2+Si-TRPV6
Q1-UL(0.92%)
Q1-UR(2.46%)
Q1-LL(94.47%)
Q1-LR(2.15%)
Q1-UL(1.61%)
Q1-UR(9.29%)
Q1-LL(86.41%)
Q1-LR(2.69%)
Q1-UL(0.75%)
Q1-UR(5.76%)
Q1-LL(91.57%)
Q1-LR(1.92%)
PI ECD-A
FITC-A
B
Apoptosis Ratio (%)
Control
E2
E2+Si-TRPV6
C
Control
E2
E2+Si-TRPV6
D
Relative Fluorescence (%)
E
Caspase-3 activity
F
Bcl2
Bax
β-actin
28kDa
20kDa
50kDa
Relative Bcl2/Bax Ratio
G
Control
E2
E2+Si-TRPV6
Tunel
DAPI
Merge

Figure4. E2 promotes osteoclasts apoptosis by increasing TRPV6 expression

(A) Apoptotic progression was monitored via flow cytometric analysis of phosphatidylserine exposure and plasma membrane integrity.

(B) The results of flow cytometric analysis are shown as percentages of positive. n = 3, **p<0.01.

(C and D) Intracellular Ca^{2+} levels were measured in terms of relative fluorescence using Fluo-4AM. Estrogen treatment significantly decreased the levels of intracellular Ca^{2+}, but this decrease was attenuated for cells where Trpv6 was silenced. n = 3, **p<0.01. Scale bars, 10 μm.

(E) Caspase-3 activity was measured in cells treated with or without estrogen for 48 h and transfection with lentivirus-siRNA targeting TRPV6. n = 3, *p<0.05, **p<0.01.

(F) BCL2 and BAX proteins were analyzed by western blot for cells treated with or without estrogen for 48 h and transfection with lentivirus-siRNA targeting TRPV6. n = 5, F = 58.51, *p<0.05, **p<0.01.

(G) Cell apoptosis was detected by Hoechst 33342 staining in cells treated with or without estrogen and transfection with lentivirus-siRNA targeting TRPV6. Scale bars, 20 μm.

(B, D, and E) Results illustrate median of n = 3. Statistical differences were determined by Kruskal-Wallis test and corrected for multiple testing by Bonferroni. Only statistically significant differences are illustrated. *p<0.05, **p<0.01. (F) Results illustrate mean ± SD of n = 5. Statistical differences were determined by one-way ANOVAs and corrected for multiple testing using the Tukey method. Only statistically significant differences are illustrated. *p<0.05, **p<0.01.

osteoclasts, whereas E2 deficiency inhibits TRPV6 expression in osteoclasts. These findings indicate that E2 may affect the long-term function of Ca^{2+} signaling through increased TRPV6 expression, leading to sustained oscillatory Ca^{2+} changes, which in turn regulate osteoclast differentiation.

Previous studies have reported that E2 affects osteoclast function by regulating osteoclastogenesis to reduce bone resorption and induce osteoclast apoptosis (Song et al., 2018; Sorensen et al., 2006; Kim et al., 2020). We found that TRPV6 silencing attenuates the inhibitory effect of E2 on osteoclast differentiation and fusion and that E2 stimulates osteoclast apoptosis by increasing TRPV6 expression. Our results strongly suggest that TRPV6 mediates the regulatory effect of E2 on bone resorption and osteoclast apoptosis. With regard to the molecular mechanism, it has been postulated that the kinetics of ERK phosphorylation and the length of time that phospho-ERKs are retained in the cell nucleus determine the pro- or antiapoptotic effects of E2, with the transient activation of the MAPK/ERK pathway associated with induced antiapoptotic effects (Chen et al., 2005). Consistent with these previous findings, we found that TRPV6 induces osteoclast apoptosis by inhibiting the MAPK-ERK pathway. Our results thus extend our understanding of the mechanisms by which E2 promotes apoptosis in osteoclasts.

Classical ER signaling is crucial for the development of the murine male skeleton (Condliffe et al., 2001). There are two related receptors mediating the effects of E2, ERα and Erβ (Spelsberg et al., 1999). Vidal et al. (2000) first demonstrated that the important effect of E2 on bone metabolism in male mice is mediated via its interactions with ERα but not ERβ. Sims found that ERβ deficiency did not affect bone metabolism in mice, whereas loss of ERα led to decreases in cortical density and thickness (Sims et al., 2002). Consistent with this previous research, we found that the regulatory effect of E2 on TPRV6 expression in osteoclasts is primarily mediated by ERα, not ERβ. Our results further strengthen the conclusion that ERα plays a crucial role in E2-mediated bone metabolism.

Previous studies reported that the classical genomic pathway and the non-classical genomic pathway are two main pathways by which E2 regulates the target gene transcription after binding to its receptor. The classical genomic pathway involves direct DNA binding of E2-ER to estrogen response elements (EREs) (Song et al., 2018; Beato et al., 1995). The alternate, non-classical genomic pathway involves the indirect modulation of transcription by the interaction of ER with other transcription complexes, such as AP-1, C/EBPβ, and NF-κB (Cong et al., 2014; Cheng and de Groat, 2014). Using computer software, we found that there was no ERE in the promoter region of mouse *Trpv6* gene, indicating that the classical genomic pathway may not be involved in the regulation of TRPV6 expression by E2-liganded ER. However, there were several C/EBPβ and NF-κB response elements in the promoter region of the mouse *Trpv6* gene. In addition, the current study revealed that the C/EBPβ-binding sites are mainly located at the −1,866 nt to −1,761 nt and −2,685 nt to −2,580 nt fragments of the Trpv6 promoter, whereas NF-κB-binding sites are mainly located in the 953 nt to -851 nt fragment of the Trpv6 promoter.

In conclusion, our study provides new evidence that TRPV6 plays a dominant role in E2-mediated osteoclast formation, bone resorption activity, and osteoclast apoptosis. Furthermore, this study provides new insights into the molecular mechanisms by which E2 up-regulates TRPV6 expression in osteoclasts, which may offer a specific and powerful therapeutic target for treatment of bone loss caused by E2 deficiency.

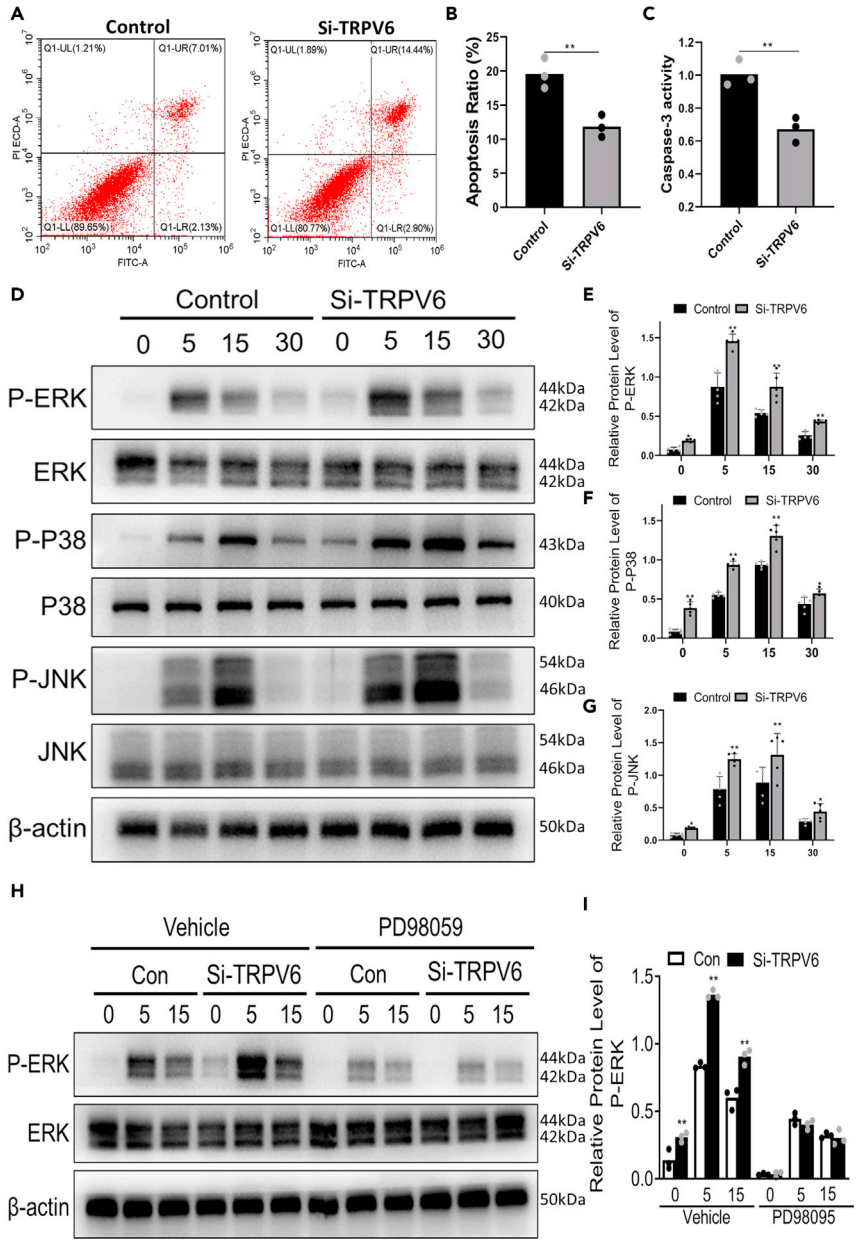

Figure5. TRPV6 induces osteoclast apoptosis by inhibiting the MAPK-ERK pathway

(A) Apoptotic progression was monitored via flow cytometric analysis of PS exposure and plasma membrane integrity.

(B) The results of flow cytometric analysis are shown as percentages of positive. n = 3, **p<0.01.

(C) Caspase-3 activity was measured in cells infected with Lenti-SiRNA-TRPV6. n = 3, **p<0.01.

(D) At 0, 5, 15, and 30 min of treatment with RANKL, cells were harvested and analyzed by western blotting using anti-ERK, anti-pERK, anti-P38, anti-pP38, anti-JNK, anti-pJNK, and anti-actin antibodies.

(E–G) Quantitative analysis showed that the ratio of p-ERK/ERK, p-P38/P38, and p-JNK/JNK was increased in cells transfected with lentivirus-siRNA targeting TRPV6. n = 5, *p< 0.05, **p<0.01.

(H and I) After PD98059 blocking the MAPK-ERK pathway, western blotting revealed that there was no significant difference in the expression level of p-ERK/ERK between the osteoclast infected with Lenti-siRNA-TRPV6 or not. n = 3, *p< 0.05, **p<0.01.

(B, C, and I) Results illustrate median of n = 3. Statistical differences were determined by Wilcoxon rank sum tests. Only statistically significant differences are illustrated. **p<0.01. (E, F, G) Results illustrate mean ± SD of n = 5. Statistical differences were determined by one-way ANOVAs and corrected for multiple testing using the Tukey method. Only statistically significant differences are illustrated. *p< 0.05, **p<0.01.

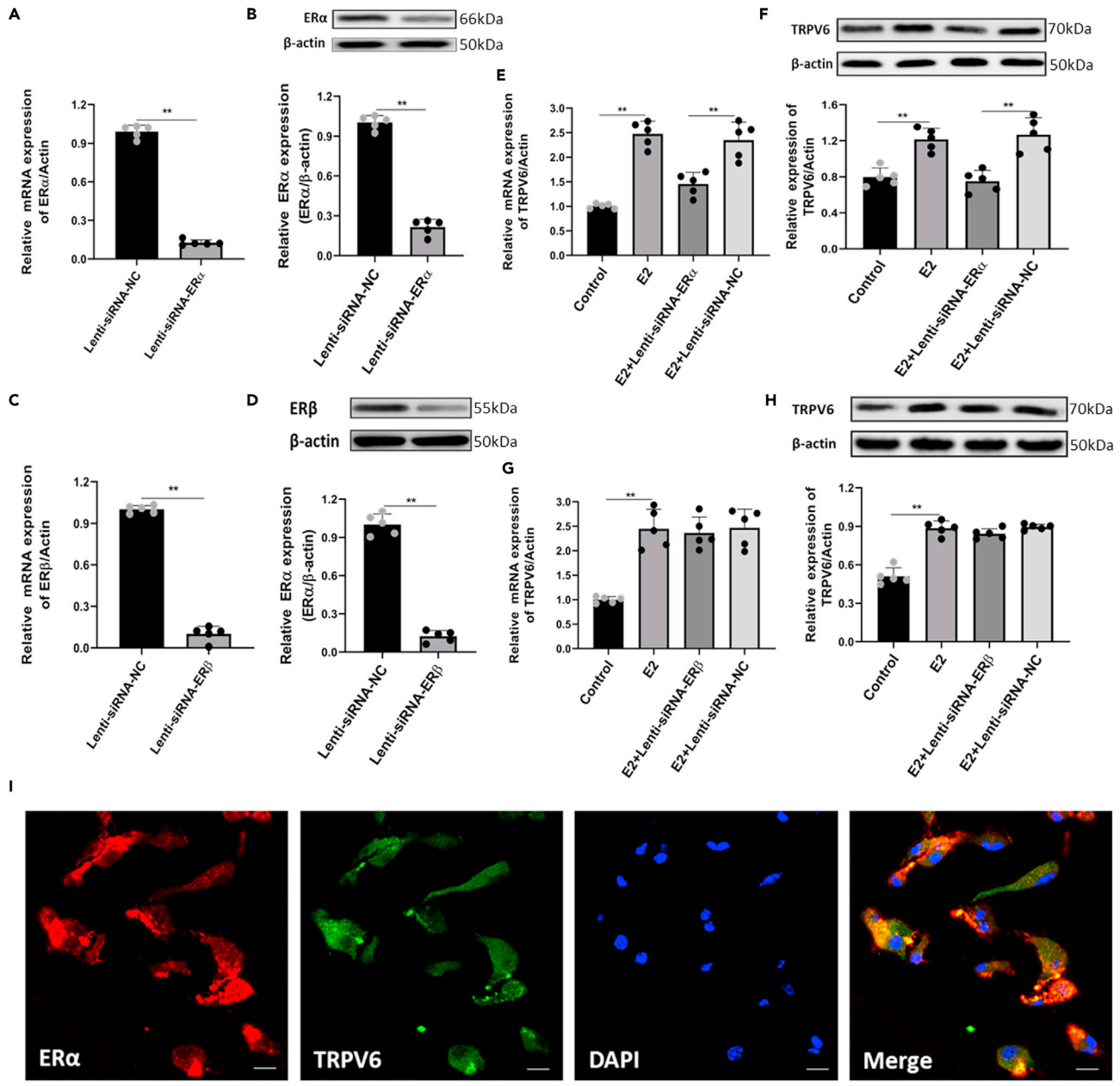

Figure6. ERα is involved in the regulation of TRPV6 expression by E2

(A and B) Verified the ERα knockdown effect by lentivirus-mediated transduction of osteoclast. n = 5, **p< 0.01.

(C and D) Verified the ERβ knockdown effect by lentivirus-mediated transduction of osteoclast. n = 5, **p< 0.01.

(E and F) TRPV6 expression was measured by real-time RT-PCR (E) and western blot (F) in osteoclast treated with E2 and infected with Lenti-siRNA-ERα under RANKL for 48 h. n = 5, **p<0.01.

(G and H) TRPV6 expression was measured by real-time RT-PCR (G) and western blot (H) in osteoclast treated with E2 and infected with Lenti-siRNA-ERβ under RANKL for 48 h. n = 5, **p<0 .01.

(I) Immunofluorescence images of ERα and TRPV6 in osteoclast induction with RANKL. Scale bars, 50 μm.

(A–D) Results illustrate mean ± SD of n = 5. Statistical differences were determined by two-tailed non-paired Student's t test. Only statistically significant differences are illustrated. **p<0.01. (E–H) Results illustrate mean ± SD of n = 5. Statistical differences were determined by one-way ANOVAs and corrected for multiple testing using the Tukey method. Only statistically significant differences are illustrated. **p<0.01.

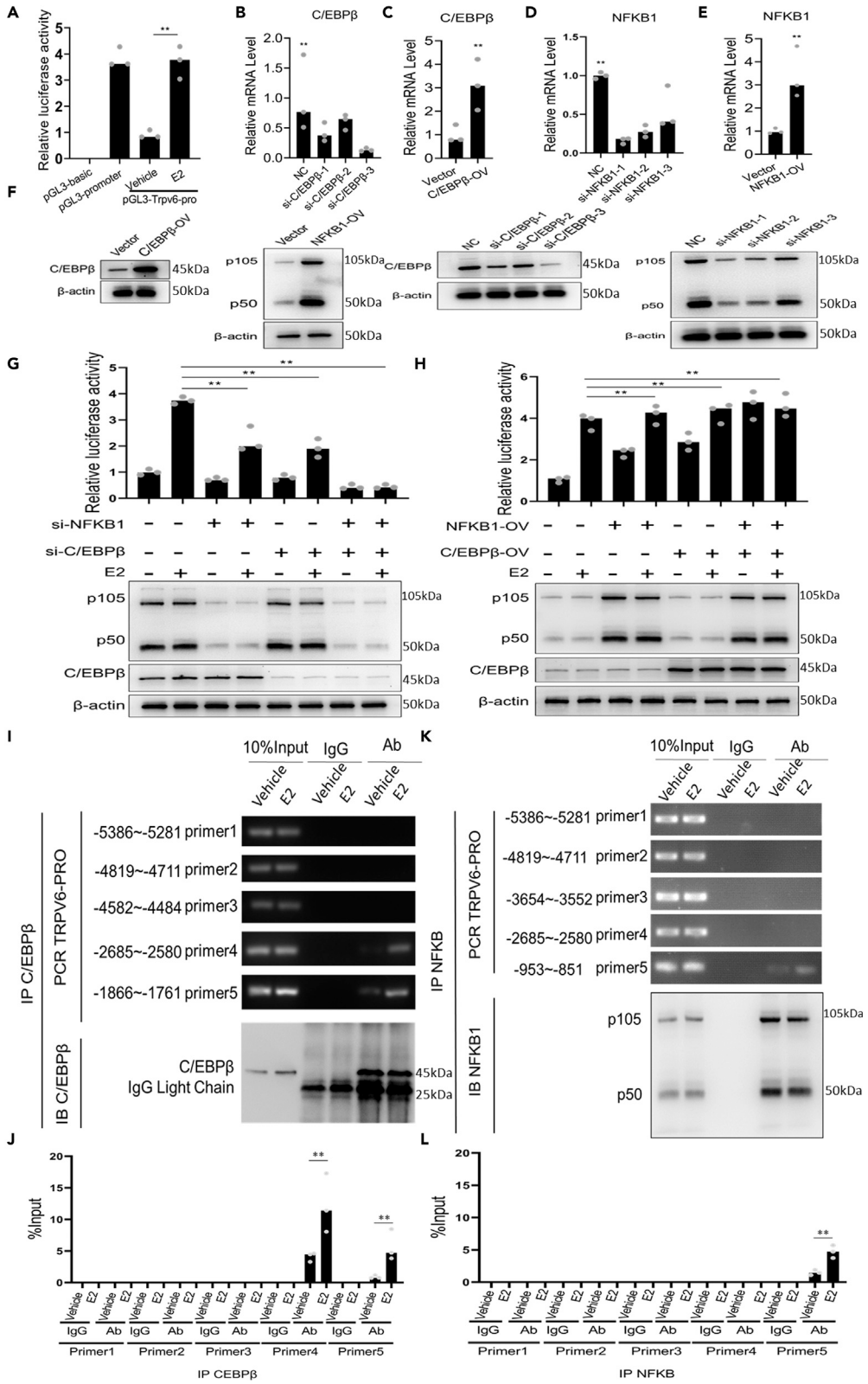
A
Relative luciferase activity
pGL3-basic
pGL3-promoter
Vehicle
E2
pGL3-Trpv6-pro
B
C/EBPβ
Relative mRNA Level
NC
si-C/EBPβ-1
si-C/EBPβ-2
si-C/EBPβ-3
C
C/EBPβ
Relative mRNA Level
Vector
C/EBPβ-OV
D
NFKB1
Relative mRNA Level
NC
si-NFKB1-1
si-NFKB1-2
si-NFKB1-3
E
NFKB1
Relative mRNA Level
Vector
NFKB1-OV
F
Vector
C/EBPβ-OV
C/EBPβ
β-actin
45kDa
50kDa
Vector
NFKB1-OV
p105
p50
β-actin
105kDa
50kDa
NC
si-C/EBPβ-1
si-C/EBPβ-2
si-C/EBPβ-3
C/EBPβ
β-actin
45kDa
50kDa
NC
si-NFKB1-1
si-NFKB1-2
si-NFKB1-3
p105
p50
β-actin
105kDa
50kDa
G
Relative luciferase activity
si-NFKB1
si-C/EBPβ
E2
p105
p50
C/EBPβ
β-actin
105kDa
50kDa
45kDa
50kDa
H
Relative luciferase activity
NFKB1-OV
C/EBPβ-OV
E2
p105
p50
C/EBPβ
β-actin
105kDa
50kDa
45kDa
50kDa
I
10%Input
IgG
Ab
Vehicle
E2
IP C/EBPβ
PCR TRPV6-PRO
-5386~-5281 primer1
-4819~-4711 primer2
-4582~-4484 primer3
-2685~-2580 primer4
-1866~-1761 primer5
IB C/EBPβ
C/EBPβ
IgG Light Chain
45kDa
25kDa
IP NFKB
K
10%Input
IgG
Ab
Vehicle
E2
PCR TRPV6-PRO
-5386~-5281 primer1
-4819~-4711 primer2
-3654~-3552 primer3
-2685~-2580 primer4
-953~-851 primer5
IB NFKB1
p105
p50
105kDa
50kDa
J
%Input
IgG
Ab
Primer1
Primer2
Primer3
Primer4
Primer5
IP CEBPβ
L
%Input
IgG
Ab
Primer1
Primer2
Primer3
Primer4
Primer5
IP NFKB

Figure7. TRPV6 is regulated by the transcription factor C/EBPβ and NF-κB

(A) Serial truncations of the trpv6 promoter were cloned into the pGL3-basic vector, and these constructs were transfected into osteoclasts. After that, cells were treated with E2 for 48 h and luciferase activity was measured. n = 3, **p<0.01.

(B–E) QT-PCR verified the C/EBPβ and NF-κB knockdown or overexpression effect by lentivirus-mediated transduction of osteoclast. n = 3, **p<0.01.

(F) Western blot verified the C/EBPβ and NF-κB knockdown or overexpression effect by lentivirus-mediated transduction of osteoclast. n = 3, **p< 0.01.

(G) Luciferase activity was measured after treatment with E2 for 48 h. The results showed that C/EBPβ and NF-κB knockdown significantly reduced luciferase activity. n = 3, **p< 0.01.

(H) Luciferase activity was measured after treatment with E2. C/EBPβ and NF-κB overexpression significantly increased luciferase activity. n = 3, **p< 0.01.

(I and J) Chromatin immunoprecipitation (ChIP) assay shows that C/EBPβ directly binds the site located at −1,866 nt to -1,761 nt and −2 685 nt to -2,580 nt fragments on the trpv6 promoter in osteoclast. n = 3, **p< 0.01.

(K and L) ChIP assay shows that NF-κB directly binds the site located at −953 nt to -851 nt on the trpv6 promoter in osteoclast. n = 3, **p< 0.01.

(A, B, D, G, and H) Results illustrate median of n = 3. Statistical differences were determined by Kruskal-Wallis test and corrected for multiple testing by Bonferroni. Only statistically significant differences are illustrated **p<0.01. (C, E, J, and L) Results illustrate median of n = 3. Statistical differences were determined by Kruskal-Wallis test. Only statistically significant differences are illustrated **p<0.01.

Limitations of the study

Further experiments are required to prove the pathophysiological relevance of these findings in clinical research.

STATEMENT

8-week-old C57BL/6J female mice and neonatal mice were housed at the Laboratory Animal Center of the Second Military Medical University. All experiments were approved by the Medical Ethics Committee of the Second Military Medical University.

STAR★METHODS

Detailed methods are provided in the online version of this paper and include the following:

- KEY RESOURCES TABLE
- RESOURCE AVAILABILITY
  - Lead contact
  - Materials availability
  - Data and code availability
- EXPERIMENTAL MODEL AND SUBJECT DETAILS
  - Animal studies
  - Cell culture
- METHOD DETAILS
  - Skeletal phenotyping
  - Histological analysis
  - Measurements of plasma Estrogen, ALP and CTX-1
  - Rhodamine phalloidin and Tartrate-resistant acid phosphatase staining
  - Annexin V-Fluorescein isothiocyanate/propidium iodide double staining assay
  - Estimation of intracellular Ca^{2+} levels
  - Measurement of caspase-3 activity
  - Cell immunofluorescence
  - Lentiviral transduction and oligonucleotide transfection
  - Quantification of mRNA and qPCR
  - Western blot analysis
- QUANTIFICATION AND STATISTICAL ANALYSIS

SUPPLEMENTAL INFORMATION

Supplemental information can be found online at https://doi.org/10.1016/j.isci.2021.103261.

ACKNOWLEDGMENTS

We thank Lei Guo (SJTU, Shanghai) and Aimin Chen (SMMU, Shanghai) for critical reading of the manuscript and help. We thank Xiaofei Ye (SMMU, Shanghai), Qi Chen (SMMU, Shanghai), Wenguang Yang (Marsh, Shanghai) for reagents and/or technical help. This study was sponsored by the National Natural Science Foundation of China (No. 81672202 and No.82102624), China Postdoctoral Science Foundation Funded Project (No. 48070).

AUTHOR CONTRIBUTIONS

J.M., conception and design, collection and assembly of data, data analysis and interpretation, manuscript writing; J.L. and Z.Z., collection and/or assembly of data, data analysis; N.L., data analysis; J.H., L.Z., conception and design, data analysis and interpretation, financial support, manuscript writing; T.Y., conception and design, data analysis and interpretation, financial support, manuscript writing, final approval of manuscript. All authors read and approved the final manuscript.

DECLARATION OF INTERESTS

The authors declare no competing interests.

Received: November 23, 2020
Revised: May 20, 2021
Accepted: October 11, 2021
Published: November 19, 2021

REFERENCES

Barthel, T.K., Mathern, D.R., Whitfield, G.K., Haussler, C.A., Hopper, H.A., Hsieh, J.C., Slater, S.A., Hsieh, G., Kaczmarska, M., Jurutka, P.W., et al. (2007). 1,25-Dihydroxyvitamin D3/VDR-mediated induction of FGF23 as well as transcriptional control of other bone anabolic and catabolic genes that orchestrate the regulation of phosphate and calcium mineral metabolism. J. Steroid Biochem. Mol. Biol. *103*, 381–388.

Bary, E.L. (2000). Expression of mRNA for the alpha 1 subunit of voltage-gated calcium channels in human osteoblast-like cell lines and normal human osteoblasts. Calcif Tissue Int. *66*, 145–150.

Beato, M., Herrlich, P., and Schutz, G. (1995). Steroid hormone receptors: many actors in search of a plot. Cell *83*, 851–857.

Beggs, R., Lee, J., Busch, K., Raza, A., Dimke, H., Weissgerber, P., Engel, J., Flockerzi, V., and Alexander, R.T. (2019). TRPV6 and Ca1.3 mediate distal small intestine calcium absorption before weaning. Cell Mol. Gastroenterol. Hepatol. *8*, 625–642.

Chen, J.R., Plotkin, L.I., Aguirre, J.I., Han, L., Jilka, R., Kousteni, S., Bellido, T., and Manolagas, S.C. (2005). Transient versus sustained phosphorylation and nuclear accumulation of ERKs underlie anti- versus pro-apoptotic effects of estrogens. J. Biol.Chem. *280*, 4632–4638.

Chamoux, E., Bisson, M., Payet, M.D., and Roux, S. (2010). TRPV-5 mediates a receptor activator of NF-kappaB (RANK) ligand-induced increase in cytosolic Ca2+ in human osteoclasts and down-regulates bone resorption. J. Biol.Chem. *285*, 25354–25362.

Chen, F., Ni, B., Yang, Y.O., Ye, T., and Chen, A. (2014a). Knockout of TRPV6 causes osteopenia in mice by increasing osteoclastic differentiation and activity. Cell Physiol. Biochem. *33*, 796–809.

Chen, F., Ouyang, Y., Ye, T., Ni, B., and Chen, A. (2014b). Estrogen inhibits RANKLinduced osteoclastic differentiation by increasing the expression of TRPV5 channel. J. Cell Biochem. *115*, 651–658.

Cheng, C.L., and de Groat, W.C. (2014). Effects of agonists for estrogen receptor α and β on ovariectomy-induced lower urinary tract dysfunction in the rat. Am. J. Physiol. Renal. Physiol *306*, 181–187.

Condliffe, S.B., Doolan, C.M., and Harvey, B.J. (2001). 17beta-oestradiol acutely regulates Cl-secretion in rat distal colonic epithelium. J.Physiol. *530*, 47–54.

Cong, B., Xu, Y., Sheng, H., Zhu, X., Wang, L., Zhao, W., Tang, Z., Lu, J., and Ni, X. (2014). Cardioprotection of 17beta-estradiol against hypoxia/reoxygenation in cardiomyocytes is partly through up-regulation of CRH receptor type 2. Mol. Cell Endocrinol. *382*, 17–25.

Denger, S., Reid, G., and Gannon, F. (2008). Expression of the estrogen receptor during differentiation of human osteoclasts. Steroids *73*, 765–774.

van der Eerden, B.C.J., Hoenderop, J.G.J., de Vries, T.J., Schoenmaker, T., Buurman, C.J., Uitterlinden, A.G., Pols, H.A.P., Bindels, R.J.M., van Leeuwen, J.P.T.M., et al. (2005). The epithelial Ca2+ channel TRPV5 is essential for proper osteoclastic bone resorption. Proc. Natl. Acad. Sci. U S A *102*, 17507–17512.

van der Eerden, B.C., Weissgerber, P., Fratzl-Zelman, N., Olausson, J., Hoenderop, J.G.J., Schreuders-Koedam, M., Eijken, M., Roschger, P., Vries, T.J.D., Chiba, H., et al. (2012). The transient receptor potential channel TRPV6 is dynamically expressed in bone cells but is not crucial for bone mineralization in mice. J. CellPhysiol. *227*, 1951–1959.

Hasegawa, H., Kido, S., Tomomura, M., Fujimoto, K., Hasegawa, H., Kido, S., Tomomura, M., Fujimoto, K., Ohi, M., Kiyomura, M., Kanegae, H., Inaba, A., Sakagami, H., and Tomomura, A. (2010). Serum calcium-decreasing factor, caldecrin, inhibits osteoclast differentiation by suppression of nfatc1 activity. J. Biol.Chem. *285*, 25448–25457.

Hemmatian, H., Bakker, A.D., Klein-Nulend, J., and van Lenthe, G.H. (2017). Aging, osteocytes, and mechanotransduction. Curr.Osteoporos.Rep. *15*, 401–411.

Ikebuchi, Y., Aoki, S., Honma, M., Hayashi, M., Sugamori, Y., Khan, M., Kariya, Y., Kato, G., Tabata, Y., Penninger, J.M., et al. (2018). Coupling of bone resorption and formation by RANKL reverse signalling. Nature *561*, 195–200.

Jeong, E., Choi, H.K., Park, J.H., and Lee, S.Y. (2018). STAC2 negatively regulates osteoclast formation by targeting the RANK signaling complex. Cell Death Differ. *25*, 1364–1374.

Karsenty, G. (2006). Convergence between bone and energy homeostases: Leptin regulation of bone mass. Cell Metab. *4*, 341–348.

Kim, M.S., Yang, Y.M., Son, A., Tian, Y.S., Lee, S.I., Kang, S.W., Muallem, S., and Shin, D.M. (2010). Rankl-mediated reactive oxygen species pathway that induces long lasting Ca2+ oscillations essential for osteoclastogenesis. J. Biol. Chem. *285*, 6913–6921.

Kim, H.N., Ponte, F., Nookaew, I., Ucer Ozgurel, S., Marques Carvalho, A., Lyer, S., and Warren, A. (2020). Estrogens decrease osteoclast number by

attenuating mitochondria oxidative phosphorylation and ATP production in early osteoclast precursors. Sci. Rep. *10*, 1–17.

Klein-Nulend, J., van Oers, R.F., Bakker, A.D., and Bacabac, R.G. (2015). Bone cell mechanosensitivity, estrogen deficiency, and osteoporosis. J. Biomech. *48*, 855–865.

Kong, Y.Y., Yoshida, H., Sarosi, I., Tan, H.L., Timms, E., Capparelli, C., Morony, S., Oliveira-dos-Santos, A.J., Van, G., Khoo, W., et al. (1999). Opgl is a key regulator of osteoclastogenesis lymphocyte development and lymph-node organogenesis. Nature *397*, 315–323.

Kuroda, Y., Hisatsune, C., Nakamura, T., Matsuo, K., and Mikoshiba, K. (2008). Osteoblasts induce Ca2+ oscillation-independent NFATc1 activation during osteoclastogenesis. Proc. Natl. Acad. Sci. U S A *105*, 8643–8648.

Lieben, L., Benn, B.S., Ajibade, D., Stockmans, I., Moermans, K., Hediger, M.A., Peng, J.B., Christakos, S., Bouillon, R., and Carmeliet, G. (2010). Trpv6 mediates intestinal calcium absorption during calcium restriction and contributes to bone homeostasis. Bone *47*, 301–308.

Ma, J., Fu, Q., Wang, Z., Zhou, P., Qiang, S.C., Wang, B., and Chen, A.M. (2019). Sodium hydrosulfide mitigates dexamethasone-induced osteoblast dysfunction by interfering with mitochondrial function. Biotechnol. Appl. Biochem. *66*, 690–697.

Ma, J., Zhu, L., Zhou, Z., Song, T., Yang, L., Yan, X., Chen, A., and Ye, T.W. (2021). The calcium channel TRPV6 is a novel regulator of RANKL induced osteoclastic differentiation and bone absorption activity through the IGF–PI3K–AKT pathway. Cell Prolif. *54*, e12955.

Manolagas, S.C., O'Brien, C.A., and Almeida, M. (2013). The role of estrogen and androgen receptors in bone health and disease. Nat. Rev. Endocrinol. *9*, 699–712.

Masuyama, R., Vriens, J., Voets, T., Karashima, Y., Owsianik, G., Vennekens, R., Lieben, L., Torrekens, S., Moermans, K., and Bosch, A.V. (2008). Trpv4-mediated calcium influx regulates terminal differentiation of osteoclasts. Cell Metab. *8*, 257–265.

Mundy, G.R. (2007). Osteoporosis and inflammation. Nutr. Rev. *65*, 147–151.

Schoeber, J.P., Hoenderop, J.G., and Bindels, R.J. (2007). Concerted action of associated proteins in the regulation of TRPV5 and TRPV6. Biochem.Soc. Trans. *35*, 115–119.

Shevde, N.K., Bendixen, A.C., Dienger, K.M., and Pike, J.W. (2000). Estrogens suppressRANK ligand-induced osteoclast differentiation via a stromal cell independent mechanism involving c-Jun repression. Proc. Natl. Acad. Sci. U S A *97*, 7829–7834.

Sims, N.A., Dupont, S., Krust, A., Clement-LaCroix, P., Minet, D., Resche-Rigon, M.,

Gaillard-Kelly, M., and Baron, R. (2002). Deletion of estrogen receptors reveals a regulatory role for estrogen receptors _ in bone remodeling in females but not in males. Bone *30*, 18–25.

Song, T., Lin, T., Ma, J., Guo, L., Zhang, L., Zhou, X.H., and Ye, T.W. (2018). Regulation of TRPV5 transcription and expression by E2/ERa signalling contributes to inhibition of osteoclastogenesis. J. Cell Mol. Med. *22*, 4738–4750.

Sorensen, M.G., Henriksen, K., Dziegiel, M.H., Tanko, L.B., and Karsdal, M.A. (2006). Estrogen directly attenuates human osteoclastogenesis, but has no effect on resorption by mature osteoclasts. DNA Cell Biol. *25*, 475–483.

Spelsberg, T.C., Subramaniam, M., Riggs, B.L., and Khosla, S. (1999). The actions and interactions of sex steroids and growth factors/cytokines on the skeleton. Mol. Endocrinol. *13*, 819–828.

Teitelbaum, S.L. (2000). Bone resorption by 0steoclasts. Science *289*, 1504–1508.

Vidal, O., Lindberg, M.K., Hollberg, K., Baylink, D.J., Andersson, G., Lubahn, D.B., Mohan, S., Gustafsson, J., and Ohlsson, C. (2000). Estrogen receptor specificity in the regulation of skeletal growth and maturation in male mice. Proc. Natl. Acad. Sci. U S A *97*, 5474–5479.

STAR★METHODS

KEY RESOURCES TABLE

REAGENT or RESOURCE	SOURCE	IDENTIFIER
Antibodies		
Anti-TRPV6	Invitrogen	AB_2736752
Anti-pJNK	Invitrogen	AB_2532273
Anti-JNK	Invitrogen	AB_2533724
Anti-Bcl2	Invitrogen	AB_10978135
Anti-Bax	Invitrogen	AB_2533132
Anti-pERK	Invitrogen	AB_2533719
Anti-ERK	Invitrogen	AB_2533024
Anti-pP38 MAPK	Invitrogen	AB_2533721
Anti-P38 MAPK	Invitrogen	AB_2533144
Anti-Estrogen receptor α	Invitrogen	AB_11002193
Anti-Estrogen receptor β	Invitrogen	AB_325597
Anti-C/EBP β	Invitrogen	AB_2078054
Anti-NFKB1 p50	Invitrogen	AB_2533906
Anti-NFKB1 p105	Invitrogen	AB_2792435
Biological samples		
Female,8-week-old, C57BL/6J mice	Laboratory Animal Center of the Second Military Medical University	NA
Neonatal C57BL/6J mice	Laboratory Animal Center of the Second Military Medical University	NA
Chemicals, peptides, and recombinant proteins		
paraformaldehyde	Aladdin	CAS:30525-89-4
EDTA buffered saline	Aladdin	CAS:60-00-4
a-MEM medium	Invitrogen	NA
M-CSF	Peprotech	NA
RANKL	Peprotech	NA
V–FITC/PI Kit	Sigema	NA
ELISA kits	Mlbio	NA
Fluo-4AM calcium assay kit	MCE	NA
Oligonucleotides		
Primesr: TRPV6 (RT-PCR) CCCAAGCTTATTTTACTGAATTCT (forward) CGGGGTACCCTAGTAGGCCCAG (reverse)	IDT	NM_022413
Primesr: CathepsinK(RT-PCR) GAAGAAGACTCACCAGAAGCAG (forward) TCCAGGTTATGGGCAGAGATT (reverse)	IDT	NM_007802
Primesr: TRAP(RT-PCR) CACTCCCACCCTGAGATTTGT (forward) CATCGTCTGCACGGTTCTG (reverse)	IDT	NM_001355189
Primesr: Atp6v0d2(RT-PCR) TGCGGCAGGCTCTATCCAGAGG (forward) CCACTGCCACCGACAGCGTC (reverse)	IDT	NM_175406

(*Continued on next page*)

Continued

REAGENT or RESOURCE	SOURCE	IDENTIFIER
Primesr: DC-STAMP(RT-PCR) GGGGACTTATGTGTTTCCACG (forward) ACAAAGCAACAGACTCCCAAAT (reverse)	IDT	NM_029422
Primesr: Erα(RT-PCR) CCCGCCTTCTACAGGTCTAAT (forward) CTTTCTCGTTACTGCTGGACAG (reverse)	IDT	NM_007956
Primesr: Erβ(RT-PCR) CTGTGATGAACTACAGTGTTCCC (forward) CACATTTGGGCTTGCAGTCTG (reverse)	IDT	NM_010157
Primesr: C/EBPβ(RT-PCR) AATCCGGATCAAACGTGGCT (forward) TGCTCGAAACGGAAAAGGTTC (reverse)	IDT	NM_001287739
Primesr: NF-κB(RT-PCR) ATGGCAGACGATGATCCCTAC (forward) CGGAATCGAAATCCCCTCTGTT (reverse)	IDT	NM_008689
Primesr: β-actin(RT-PCR) GGCTGTATTCCCCTCCATCG (forward) CCAGTTGGTAACAATGCCATGT (reverse)	IDT	NM_173979
Software and algorithms		
Statistics: Prism 8.0	GraphPad	https://www.graphpad.com/scientific-software/prism/
Fiji	ImageJ	https://imagej.net/Fiji

RESOURCE AVAILABILITY

Lead contact

Requests for further information and reagents should be directed to and will be fulfilled by the Lead Contact Tianwen Ye(yetianwenvip@126.com).

Materials availability

Materials generated in this study will be made available upon reasonable request and may require a material transfer agreement.

Data and code availability

Data: All data produced or analyzed for this study are included in the published article and its supplementary files or are available from the corresponding author upon reasonable request.

Code: This paper does not report original code.

Other items: Any additional information required to reanalyze the data reported in this paper is available from the lead contact upon request.

EXPERIMENTAL MODEL AND SUBJECT DETAILS

Animal studies

8-week-old C57BL/6J female mice (from the Laboratory Animal Center of the Second Military Medical University) were used in this study. The mice were randomly assigned in equal numbers to SHAM and ovariectomy operation (OVX) groups. The animals were housed in rearing cages (five mice per cage) and kept under standard laboratory conditions (12-h light–dark cycle; 25°C). Six weeks after operations, ovariectomized or SHAM-operated mice were anesthetized for use in experiments. Experiments were approved by the Medical Ethics Committee of the Second Military Medical University.

Cell culture

Bone marrow cells were isolated from the femur and tibiae of C57BL/6 mice. Cells were cultured in a-MEM medium (Invitrogen, Paisley, UK) supplemented with M-CSF (Peprotech, Rocky Hill, NJ, USA) for 1 day. The unadherent cells were harvested and cultured in a medium containing M-CSF (50 ng/mL) for 3 days. Then the adherent cells, which were preosteoclasts, were collected. Next, osteoclast precursors from normal mice were incubated with 10^{-8}M E2 or not for 24 h. After estrogen pretreatment, a-MEM medium containing M-CSF (30 ng/mL) and RANKL (50 ng/mL) (Peprotech, Rocky Hill, NJ, USA) was added and allowed to incubate for 7 days to generate mature osteoclasts.

METHOD DETAILS

Skeletal phenotyping

To assess bone density and trabecular micro architecture, the distal femurs were scanned using micro-computed tomographic imaging (SkyScan, Aartselaar, Belgium). The scanning analysis area was the trabecular portion of the proximal femoral growth plate from 2 mm downward.

Histological analysis

Harvested femurs were fixed in 4% paraformaldehyde solution (Aladdin, Shanghai, China) and decalcified in EDTA buffered saline solution (Aladdin, Shanghai, China). Sagittal tissue sections (10 μm thick) were prepared for immunohistochemistry, and TRAP staining was performed afterward to assess histological changes.

Measurements of plasma Estrogen, ALP and CTX-1

Plasma E2, alkaline phosphatase (ALP) and C-telopeptide of type 1 collagen (CTX-1) concentrations were determined using ELISA kits (Mlbio, Shanghai, China). Animals were fasted for 12 hours before sampling, samples were incubated for 2 h on microporous plates. Next, an equivalent volume of anti-Estrogen, anti-ALP or anti-CTX-1 primary antibody was added to each sample and incubated for another hour. This was followed by a half-hour incubation with secondary antibodies. Finally, a microplate reader was used to detect absorbance values (at 450 nm).

Rhodamine phalloidin and Tartrate-resistant acid phosphatase staining

Primary BMM cells were expanded in α-MEM with M-CSF (50 ng/mL) for 3 days to generate preosteoclasts. These cells were then seeded and further cultured with complete a-MEM medium containing M-CSF(30 ng/mL) and RANKL (50 ng/mL) for 7 days to acquire mature osteoclasts. For Rhodamine phalloidin staining, cells were fixed in 4% paraformaldehyde, followed by incubation with 0.1% Triton X for 5 min. Next, the solution was replaced with Rhodamine phalloidin solution, and cells were kept stationary in a dark room for 30 min. Confocal laser scanning microscopy (Carl Zeiss, Oberkochen, Germany) was used to detect the fluorescence signal. For Tartrate-resistant acid phosphatase staining, TRAP solution was added to the well and incubated with the cells at 37°C for 15 min. $TRAP^{+}$ cells with more than three nuclei were counted as mature osteoclasts. Three fields of view were selected for each well under an optical microscope, and the means of the cell numbers were calculated.

Annexin V-Fluorescein isothiocyanate/propidium iodide double staining assay

Osteoclast apoptosis was measured using annexin V–FITC/PI double staining assays. The annexin V-fluorescein isothiocyanate (FITC)/propidium iodide (PI) apoptosis detection kit was purchased from Sigma (St Louis, USA). Briefly, the cells were washed in 4°C PBS and resuspended in 500 μl of binding buffer. Next, cells were stained with 10 μl annexin V and 5 μl PI in the dark for 15 min at room temperature. The cells were then analyzed by flow cytometry.

Estimation of intracellular Ca^{2+} levels

The relative levels of intracellular Ca^{2+} across different culture conditions were measured using Fluo-4AM calcium assay kit (MCE, NJ, USA). The assay was performed as per manufacturer's instructions. Values are expressed as fluorescence units (%) relative to control for each independent assay performed.

Measurement of caspase-3 activity

Caspase activities were measured with a caspase activity kit according to the manufacturer's instructions (BioVision, Mountain View, USA). The cells were washed with cold PBS, resuspended in lysis buffer, and

left on ice for 15 min. The samples were then added to the reaction buffer containing Ac-DEVD-pNA, incubated for 2 h at 37°C. The absorbance of yellow pNA, cleaved from its corresponding precursors, was measured using a spectrometer at 405nm. The fold increase in activity was calculated as the ratio between values obtained from the treated versus the untreated controls.

Cell immunofluorescence

Bone marrow macrophage cells (BMMs) were induced by M-CSF and RANKL for 7 days. Then, the culture medium was washed with PBS and the cells were fixed with 4% paraformaldehyde for 20 min. Afterward, 0.2% Triton X-100 was applied for 5 min to permeabilize the cells. After washing away the permeabilizing solution with PBS, the permeable cells were blocked with 5% BSA for half an hour. Additionally, the primary antibodies (anti-TRPV6, anti-ERα or anti-p-AKT) were added and incubated with cells overnight at 4°C. PBS was used to wash off the primary antibodies and corresponding secondary antibodies for 30 min at 37°C. After the secondary antibody was washed away, the cells were finally fixed with an anti-fading fixing medium. Fluorescence was observed by confocal laser scanning microscopy (Leica, Germany).

Lentiviral transduction and oligonucleotide transfection

Osteoclast precursors were seeded into the 6-well plates with a density of 2×10^5 and transfection began when the cell fusion rate reached approximately 60%. Cells were infected with TRPV6 shRNA lentiviral particles or TRPV6 lentiviral activation particles (Santa Cruz, CA, USA) separately for 24 h. The culture medium was then replaced with a normal osteoclast induction medium.

Quantification of mRNA and qPCR

Total RNA was isolated from cells using TRIzol reagent (Takara Biotechnology, Japan), and cDNA was synthesized from RNA with the miScript Reverse Transcription Kit (Takara, Tokyo, Japan) according to the manufacturer's protocols. qRT-PCR was carried out with the SYBR Green PCR kit (Takara Biotechnology, Japan) and sequence detection was performed using an ABI 7500 Sequencing Detection System (Applied Biosystems, Foster City, CA). β-actin was used as the housekeeping gene.

Western blot analysis

Proteins the from osteoclast lysates were introduced to 10% SDS-PAGE and were subsequently electroblotted onto a polyvinylidene fluoride membrane. The membrane was blocked with 5% fat-free milk and incubated with appropriate antibodies. Chemiluminescence reagents (Thermo Scientific, Rockford, IL, USA) were used to detect antigen–antibody complexes. ImageJ software was used to quantify the immunoblots.

QUANTIFICATION AND STATISTICAL ANALYSIS

SPSS 24.0 statistical software was used for statistical analysis. When the sample size was equal to 5,quantitative data were assessed for normality using the Shapiro-Wilk test. The Levene test was used for examining the equality of variance (homogeneity). Normally-distributed data were reported as mean ± SD. Two-tailed non-paired Student's t-tests were used for comparisons between two groups. One-way ANOVAs were used for comparison among three or more groups, with Tukey correction for multiple testing. When the sample size was equal to 3, the average levels of data were described by median, and Wilcoxon rank sum tests were used to conduct comparison for two groups while Kruskal-Wallis test were used for three or more groups with Bonferroni correction for multiple testing. Differences were considered significant if $P < .05$, and a high-level of significance was $P < .01$.